Dimensionless argument: a narrow grain size range near 2 mm plays a special role in river sediment transport and morphodynamics

Gary Parker[1,2], Chenge An[3], Michael P Lamb[4], Marcelo H Garcia[2] Elizabeth H Dingle[5], Jeremy G Venditti[6]

[1]Department of Earth Sciences and Environmental Change, University of Illinois Urbana-Champaign, Urbana, IL 61801, USA
[2]Department of Civil and Environmental Engineering, University of Illinois Urbana-Champaign, Urbana, IL 61801, USA
[3]State Key Laboratory of Hydroscience and Engineering, Department of Hydraulic Engineering, Tsinghua University, Beijing, 100084, China.
[4]Division of Geological and Planetary Sciences, California Institute of Technology, Pasadena, CA 91125, USA
[5]Department of Geography, Durham University, South Road, Durham DH1 3LE, UK
[6]School of Environmental Science & Geography, Simon Fraser University, Burnaby, BC, V5A 1S6, Canada

Correspondence to: Gary Parker (parkerg@illinois.edu)

Abstract. The grain size 2 mm is the conventional border between sand and gravel. This size is used extensively, and generally without much physical justification, to discriminate between such features as sedimentary deposit type (clast-supported versus matrix-supported), river type (gravel-bed versus sand-bed) and sediment transport relation (gravel versus sand). Here we inquire as to whether this 2 mm boundary is simply a social construct upon which the research community has decided to agree, or whether there is some underlying physics. We use dimensionless arguments to show the following for typical conditions on Earth, i.e., natural clasts (e.g. granitic or limestone) in 20°C water. As grain size ranges from 1 to 5 mm (a narrow band including 2 mm), sediment suspension becomes vanishingly small at normal flood conditions in alluvial rivers. We refer to this range as pea gravel. We further show that bedload movement of a clast in the pea gravel range with, for example, a size of 4 mm moving over a bed of 0.4 mm particles has an enhanced relative mobility as compared to a clast with a size of 40 mm moving over a bed of the same 4 mm particles. With this in mind, we use 2 mm here as shorthand for the narrow pea gravel range of 1 – 5 mm, over which transport behaviour is distinct from both coarser and finer material. The use of viscosity allows delineation of a generalized dimensionless bed grain size discriminator between "sand-like" and "gravel-like" rivers. The discriminator is applicable to sediment transport on Titan (ice clasts in flowing methane/ethane liquid at reduced gravity) and Mars (mafic clasts in flowing water at reduced gravity) as well as Earth.

Figure 1. Clast supported versus matrix supported deposits. Clasts are > 2 mm and matrix is < 2 mm.

1 Introduction

In rivers, the grain size 2 mm is the conventional divider between sand and gravel. This size has been repeatedly used, explicitly or implicitly, as a discriminator of alluvial rivers and their deposits. For example, conglomerate deposits are often classified as clast-supported (pebble-supported) or matrix-supported, depending on whether clasts with a size in excess of 2 mm are in contact with each other (clast-supported), or whether the clasts are "floating" in a finer deposit (sand or silt: matrix-suppported): e.g. Tucker (2003), Frings (2011); Jutzeler et al. (2015); Li et al. (2017). This classification is illustrated in Figure 1.

Gravel-bed rivers (characteristic bed material size > 2 mm) and sand-bed rivers (characteristic bed material size < 2 mm) have often been treated separately. Communities of researchers have even formed around the distinction. For example, the Gravel-bed Rivers conference series has existed for nearly 40 years since early work summarized in Hey et al. (1985). Note that they specifically name their volume "Gravel-bed Rivers". This distinction has continued through at least eight successive conference proceedings (Laronne and Tsutsumi, 2018). Likewise, a large literature has been devoted exclusively to sand-bed rivers: e.g., Wright and Parker (2004), Peng et al. (2022) and Venditti and Bradley (2022). Relations for hydraulic geometry have also been derived separately for gravel-bed rivers (e.g., Parker et al., 2007; Khosravi et al., 2022) and sand-bed rivers (e.g., Xu, 2004; Wilkerson and Parker, 2011).

Many sediment transport relations have been developed exclusively for sand-bed (characteristic bed grain size < 2 mm) or gravel-bed rivers (characteristic bed grain size > 2 mm). For example, the sediment transport relation of Engelund and Hansen (1967) was developed exclusively for sand, based on the flume data of Guy et al. (1966). It was verified by Brownlie (1981), again exclusively for experiments and field data pertaining to the sand-bed case. The bedload transport relation of Meyer-Peter and Müller (1948) was originally developed exclusively using experimental results pertaining to gravel. The bedload transport relation for gravel mixtures due to Parker (1990) specifies that sand should be

a)

b)
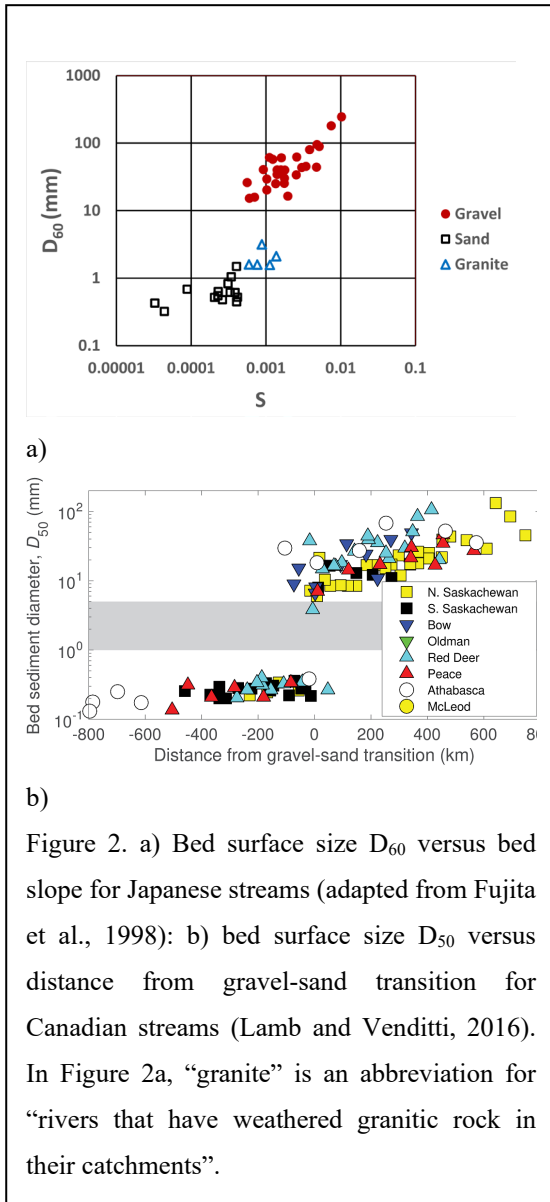
Figure 2. a) Bed surface size D_{60} versus bed slope for Japanese streams (adapted from Fujita et al., 1998): b) bed surface size D_{50} versus distance from gravel-sand transition for Canadian streams (Lamb and Venditti, 2016). In Figure 2a, "granite" is an abbreviation for "rivers that have weathered granitic rock in their catchments".

removed from the grain size distribution of the bed before the transport rate is calculated. The transport relation for sediment mixtures of Wilcock and Crowe (2003) changes the mobility of gravel (grain size D > 2 mm) depending upon the content of sand (D < 2 mm) in the bed surface material. (The bedload transport relation of Ashida and Michiue, 1972, however, does include data ranging from 0.3 mm to 7 mm. i.e., across the 2 mm size.) Experimental studies of sediment transport using size mixtures often have the size 2 mm built into experimental design; such that sediment fractions finer and coarser than this divider are allowed to interact with each other. Such studies include Hill et al. (2016) and Dingle et al (2023).

Here we pose the following questions. Is the 2 mm divider a social construct based on decades of repetition, convergence and rearticulation (as viewed from the point of view of social science: Butler, 1997), or does it have a physical basis? Why specifically 2 mm, and not 0.6 mm or 13 mm? And if the size 2 mm has a physical basis, can it be interpreted in a universal, dimensionless way?

2 Empirical evidence for 2 mm as a discriminator in alluvial rivers

There are two lines of evidence that 2 mm, or more specifically the relatively narrow range of 1 to 5 mm, plays a special role in terms of sediment transport and river morphodynamics. Different authors define this range somewhat differently: e.g., Church and Hassan (2023) use 1 – 10 mm, whereas here we follow the lead of Lamb and Venditti (2016) and define it to be 1 – 5 mm (based on the effect of viscosity described below). The most direct evidence concerns patterns of downstream fining in rivers carrying a mixture of gravel and sand. Many streams show a pattern of downstream fining such that characteristic bed surface material, e.g., median size D_{50} of the bed surface material, gradually becomes finer downstream until a size somewhat coarser than pea gravel is reached, and then abruptly declines to the range of sand. Subreaches of such streams where D_{50} is in the pea gravel range are either short (~ 5 widths) or non-existent (e,g, Sambrook Smith and Ferguson, 1995). The first person to document this behaviour was Yatsu (1955), who presented numerous abrupt gravel-sand transitions in Japanese rivers. In the Kinu River, for example, characteristic grain size drops from 20 mm to about 1 mm over a short reach. Yatsu (1955) speculates that this might be due to the abrupt shattering of granitic clasts into their component crystals when grain size is abraded to about 20 mm. Kodama (1994) provides some support of this view and emphasizes the role of abrasion. Shaw and Kellerhals (1982), however, document the same gravel-sand transition in rivers where non-crystalline sediments such as limestone dominate. Abrasion thus may not play a dominant role in the formation of abrupt gravel-sand transitions. This is further supported by observations in rivers with sharp transitions which have clasts that are highly resistant to abrasion (e.g., Ferguson et al., 1996; Venditti and Church 2014; see review in Dingle et al., 2021).

Both Fujita et al. (1996) and Lamb and Venditti (2016) use large data sets to illustrate that a substantial number of river reaches have coarse gravel beds (bed surface D_{50} or D_{60} > 5 mm) and sand beds (bed surface D_{50} or D_{60} < 1 mm),

but very few reaches have a characteristic size in the pea gravel range (Figure 2a,b). Both sets of authors cast this in the context of downstream fining and gravel-sand transitions. Fujita et al. (1996) in particular note that at least in Japan, the relatively few reaches with a characteristic bed size in the pea gravel pertain to streams with heavy loads of sediment derived from weathered granite.

Gravel-sand transitions need not be abrupt. Especially in rivers sufficiently wide to develop bedform- and planform-driven variation in local flow conditions (e.g. a bar field), the transition may be rather disperse and elongated (Frings, 2011), with interleaving of sand and coarse gravel patches for some distance downstream of the main transition (Venditti et al., 2015; Dong et al., 2016). Paola and Seal (1995) have shown how gravel-sand patchiness can drive such a transition. Frings (2011) shows this elongation of the transition region for the case the Rhine River, western Europe, where the tendency in question might be affected by anthropogenic effects such as river training. Dong et al. (2016) show this behaviour for the case of the Selenga River, Siberia, Russia, where anthropogenic effects are negligible. The transitional reaches in question often do not show substantial subreaches where pea gravel is the characteristic bed material size. Instead, that characteristic size is gravel in excess of 10 mm upstream, is below 1 mm downstream, and locally interleaves between coarser gravel and sand in the transitional region, with relatively few locations with a characteristic bed surface size in the pea gravel range. Venditti et al (2015), for example, describe the Fraser River, British Columbia as "an archetypical abrupt gravel-sand transition with a 'diffuse extension' composed of a sand bed with some patches of gravel." Dingle et al. (2021) provide a thorough review of the gravel-sand transition and grain size gap. This issue is considered in more detail in the Discussion below. Of relevance to the analysis here is the fact that both Lamb and Venditti (2016) and Dingle et al (2021) suggest a role for viscosity in regard to the grain size gap. This effect is explained in more detail below.

A second line of evidence derives from experiments with mixtures of gravel and sand. Prominent among them is the work of Wilcock and Crowe (2003), who show that in a unimodal mixture of sand and gravel, increasing content of material less than 2 mm in the bed results in an increased transport rate of material greater than 2 mm. Indeed, they modified the basic framework of the Parker (1990) relation to specifically account for this effect, which Lin et al. (2023) have described as Gravel Transport Augmenting Sand (GTAS). The results of Wilcock and Crowe (2003) have been verified by others (e.g. Cui et al, 2003a, 2003b; Dingle and Venditti, 2023). They break, however, the completely dimensionless format of Parker et al (1990) by introducing a parameter with dimensions, namely, the 2 mm cutoff between sand and gravel. We show below how this problem can be overcome.

Dingle and Venditti (2023) performed flume experiments using a bimodal mix of pea gravel (~ 3.8 mm) and sand (~ 0.57 mm) to show that the addition of sand strongly mobilizes the pea gravel. They suggest that adding sand to a bed consisting of material in the grain size gap produces a "hydraulic smoothing" effect, resulting in mobilization of material in that gap. This same effect was noted when adding sand (~ 0.57 mm) onto a broader unimodal gravel distribution (2-22 mm, D_{50} = 5.5 mm), where the pea gravel fraction became disproportionately mobile relative to the other gravel fractions. The addition of sand was found to increase gravel mobility up to a sand fraction in the bed of about 0.84,

beyond which the gravel clasts tend to get buried. Church and Hassan (2023) show experimentally how a continuous, only weakly bimodal mixture of sand and gravel can devolve into a grain size distribution with an autogenically strengthened grain size gap. They note: "Our experiment shows a clear tendency for grains in the range 1–8 mm to outrun both larger and smaller grains in the condition of size-selective transport."

3 The central problem

So what is so special about the pea gravel range? Consider a thought experiment. Loosely following Dingle and Venditti (2023), we consider Case 1, with 4 mm gravel (in the pea gravel range) moving over a 0.4 mm sand bed (finer than the pea gravel range), and Case 2, where we multiply all the numbers by 10, i.e., 40 mm gravel (coarser than the pea gravel range) moving over a 4 mm gravel bed (in the pea gravel range). Will the finer material of the bed increase the mobility of the coarser material in Case 2 to the same extent in as Case 1? We have a partial answer to this question. Venditti et al. (2010a,b) studied the case where both sizes are in the gravel range. They found that the mobility of coarse surface layers in gravel-bedded rivers could be enhanced by adding finer gravel as bedload (Case 2). The degree of enhancement, however, is not nearly as strong as Case 1 (as documented by e.g., Wilcock and Crowe, 2003). Indeed, the extra mobility of Case 2 can be explained solely in terms of the hiding-exposure functions embedded in the relations of Parker (1990) and Wilcock and Crowe (2003), as elaborated in, for example, Parker and Klingeman (1982) and Parker and Toro-Escobar (2002). These relations describe the relative mobility of different sizes in a mixture of gravel in the active (surface) layer of the bed. Relative mobility is mediated by two effects: a weight effect making coarser (and thus heavier) particles harder to move, and an exposure (hiding) effect making coarser particles more exposed to the flow and thus easier to move. The residual of the two effects (weight versus hiding-exposure effect) renders finer gravel somewhat more mobile in a sediment mix. Evidently there is something special in regard to the strong enhancement of the mobility of pea gravel moving over a sand bed (Case 1 as compared to Case 2). Here we explore two possibilities, one related to sediment suspension and one related to bedload, with both effects mediated by viscosity.

4 Pea gravel corresponds to the finest sizes that do not readily suspend in alluvial rivers

We revisit the relation of Garcia and Parker (1991) for the entrainment of bed sediment into suspension. Although the formulation includes relations for both uniform sediment and sediment size mixtures, we first consider the case of uniform sediment here. For equilibrium suspensions the relation takes the form

$$c_b = \frac{AZ_u^5}{1+\dfrac{A}{0.3}Z_u^5} \quad , \quad Z_u = \frac{u_{*s}}{v_s}\left(D^*\right)^{0.9} \quad , \quad D^* = D\frac{(Rg)^{1/3}}{v^{2/3}} \qquad (1a, b, c)$$

Here c_b is near-bed volume concentration of suspended sediment (evaluated at a point that is 5 percent of water depth above the bed), D = grain size for an equivalent sphere in terms of fall velocity, u_{*s} is bed shear velocity due to skin friction (form drag removed), v_s is particle fall velocity, g = gravitational acceleration, $R = (\rho_s - \rho)/\rho$ is the submerged specific gravity of sediment, where ρ_s = sediment density and ρ = density of the fluid in which the sediment is immersed (R ~ 1.65 for quartz in water), ν = kinematic viscosity of fluid in which the sediment is immersed, D* is a dimensionless grain size and A is a dimensionless constant given as

$$A = 1.3 \times 10^{-7} \tag{1d}$$

(The original formulation of the Garcia-Parker relation uses a particle Reynolds number $\mathbf{Re}_p = (RgD)^{1/2}D/\nu$, but is here recast in terms of the parameter $D* = (\mathbf{Re}_p)^{2/3}$, which is a more convenient representation, in so far as that dimensionless grain size D* is linearly proportional to dimensioned grain size D: van Rijn, 1984).

The Garcia-Parker (1991) relation was developed solely with experimental data on suspensions of quartz sediment in water, using a total of 62 measurements with grain size D varying from 0.093 mm to 0.44 mm, so that D* varies from 2.36 to 11.1 for quartz particles immersed in 20°C water on Earth. The relation was thus not designed to be applied to the suspension of gravel. It is nevertheless illustrative to do so.

In Figure 3a, the predictions of Equations (1a~d) are shown for the sizes D = 0.25 mm and 4.0 mm. Here these are nominal sizes using Earth parameters (g = 9.81 m/s², R = 1.65 and ν = 1x10⁻⁶ m²/s). It can be seen therein that the predictions for near-bed concentration c_b for 4 mm gravel are about half that of the corresponding values for 0.25 mm material. This seems unlikely, however: data for the suspension of any size of gravel seems to be rare in the literature, suggesting that it is suspended only with difficulty in laboratory flumes and typical alluvial river flood flows (e.g. de Leeuw et al., 2020). That is, the Garcia-Parker (1991) relation seems to overestimate the suspension of gravel, a size range which is beyond the range of the experimental data that the relation is based on.

This problem can be explained with the dimensionless fall velocity $\mathbf{R}_f$

$$\mathbf{R}_f = \frac{v_s}{\sqrt{RgD}} \tag{2}$$

The parameter $\mathbf{R}_f$ is related to dimensionless grain size D* according to. e.g., the relation of Dietrich (1982), as shown in Figure 3b (solid blue line). Also plotted on Figure 3b are the experimental data of Garcia and Parker (1991), and the dimensionless sizes D* = 25.2 and 126 (nominal sizes D = 1 mm and 5 mm for quartz particles in water on Earth). The regime to the left of nominal size D = 1 mm is viscous-dependent, i.e., dependent on D*, the regime to the right of nominal size D = 5 mm is essentially viscous-independent, and the regime of nominal sizes 1 – 5 mm defines a transitional zone. The relation defined by the solid blue line in Figure 3b is in turn derived in part from the drag relation for spheres shown in Figure 3c (e.g. Haljasmaa, 2006), in which $c_D = F_D/[(1/2)\rho\pi(D/2)^2 v_s^2]$ is a drag coefficient, where F_D denotes the drag force on a spherical particle and $\mathbf{Re}_{vp} = (v_s D/\nu)$ is a Reynolds number based on fall velocity. It is

again seen that the regime to the left of nominal size D = 1 mm is viscous-dependent, the regime to the right of nominal

190   size D = 5 mm is essentially viscous-independent (inertial regime), and the regime of nominal sizes 1 − 5 mm defines a

transitional zone.
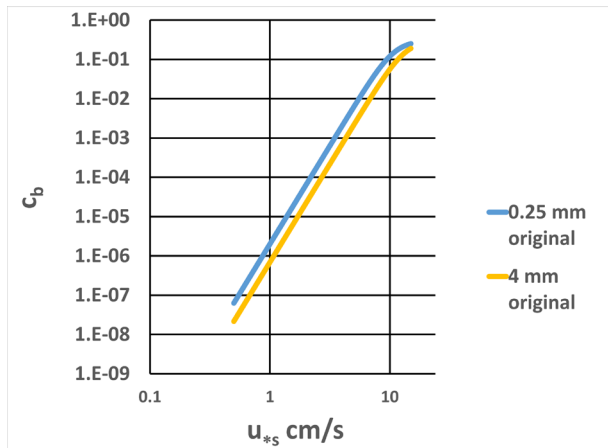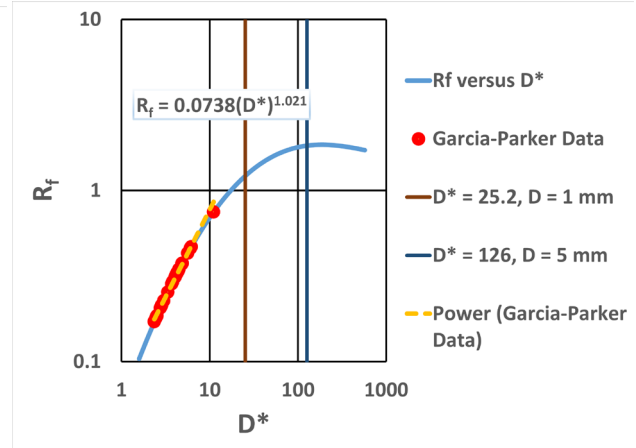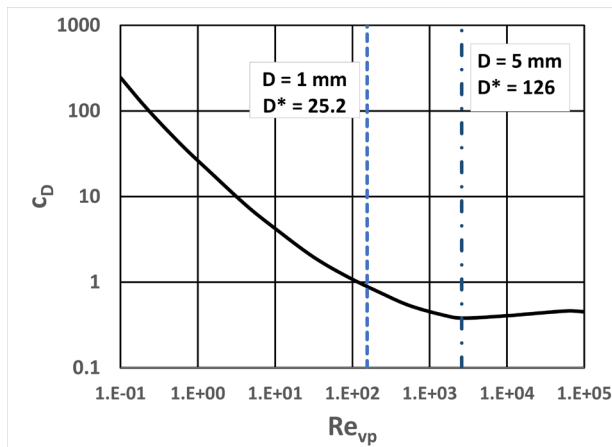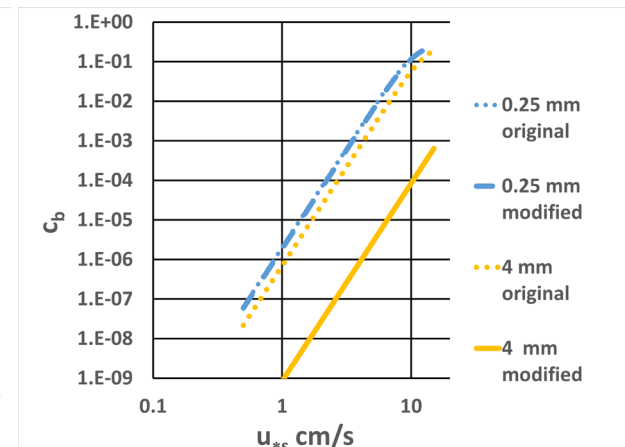
Figure 3. a) Plot of near-bed concentration of suspended load versus shear velocity due to skin friction for D = 0.25 mm and 4 mm using the original relation of Garcia and Parker (1991), i.e. Equations (1a,b,c): b) plot of dimensionless fall velocity $\mathbf{R}_f = v_s/(RgD)^{1/2}$ versus dimensionless grain size D* using the Dietrich (1982) relation (solid line), including a power regression relation for $\mathbf{R}_f$ versus D* over the original range of the data of Garcia and Parker (1991): c) drag curve for spheres illustrating viscous, transitional and inertial regimes from left to right (adapted from Haljasmaa, 2006); d) version of Figure 3a using both original (Equations 1a,b,c) corrected Equations 4a,b,c) relations for Garcia and Parker, showing near-collapse of suspension of particles of size 4 mm. In Figure 3d, the lines "0.25 mm original" and "0.25 mm modified" are on top of each other.

Figures 3b and 3c illustrate an inadequacy of the entrainment relation of Garcia and Parker (1991). The data used to derive it pertain solely to the viscous-dependent region of the relation for fall velocity, so that the relation cannot strictly be extended to coarser sizes. There is, however, a straightforward way to remedy this. Also plotted on Figure 3b (dashed line) is the following regression relation for $\mathbf{R}_f$ versus D^*, fitted specifically over the range of the data used by Garcia and Parker:

$$\mathbf{R}_f = 0.0738\left(D^*\right)^{1.021} \tag{3}$$

Figure 4. Plot of predicted values of near bed concentrations c_{bmod} using the modified formulation of Garcia and Parker (Equations 4a,b,c), versus those predicted from the original formulation, c_{borig} (Equations 1a,b,c). Calculation is conducted over the range of the Garcia-Parker data.

This relation can be substituted into Equations (1a,b,c) to yield a revised relation in which the constant A is unmodified:

$$c_b = \frac{AZ_u^5}{1+\dfrac{A}{0.3}Z_u^5} \quad , \quad Z_u = 9.95\frac{u_{*s}}{v_s}\mathbf{R}_f^{0.882} \tag{4a,b}$$

According to Equation (4b) and Figure 3b, the modified parameter Z_u does not increase without bound as dimensionless grain size D^* increases. When inertial effects dominate, $\mathbf{R}_f$ becomes roughly constant, placing a bound on Z_u and preventing the oversuspension of material in the range of pea gravel and coarser material.

Figure 4 shows that when applied over the range of the original data of Garcia and Parker (1991), the predictive power of the modified formulation of Equations. (4a,b) is as good as the original formulation of Equations (1a,b,c). Figure 3d shows that the modified formulation does not change the relation for c_b versus u_{*s} for nominal 0.25 mm quartz in water (the two lines overlap), but causes such low values of c_b for nominal 4 mm quartz in water that they are essentially negligible. This negligibility is further reinforced by the Rousean (1939) relation for vertical profile of suspended sediment concentration. This relation contains an exponent proportional to u_*/v_s, where u_* is total bed shear velocity, and so concentration above the bed collapses as v_s/u_* becomes sufficiently large.

The tendency for suspension to collapse as grain size increases across the pea gravel range can be confirmed in terms of the more recent relation of de Leeuw et al. (2020). Although several relations are presented therein, the one most directly comparable with the above formulation can be expressed in the following form for uniform material:

$$c_b = \begin{cases} \dfrac{4.74\times10^{-0.4}\,X^{1.18}}{1+3\left(4.74\times10^{-0.4}\,X^{1.18}\right)} & , \quad X>0 \\[3mm] 0 & , \quad X\le 0 \end{cases} \quad , \quad X=\left(\dfrac{u_{*s}}{v_s}\right)^{1.5}\mathbf{Fr}-0.015 \qquad (5a,b)$$

In the above relation, the Froude number $\mathbf{Fr} = U/(gH)^{1/2}$, where U is depth-averaged flow velocity and H is depth. A plot of c_b versus u_{*s} for the grain sizes D = 0.25 mm, 0.5 mm, 1 mm, 2 mm and 4 mm (quartz in water at 20°C) and Froude number $\mathbf{Fr}$ = 0.4 is given in Figure 5. It is again seen that suspension tends to collapse as grain size enters the pea gravel range. Similar results are obtained for $\mathbf{Fr}$ = 0.2 and 0.6.

The range of the parameter u_{*s} used in Figures 3a, 3d and 5 is 0 to 15 cm/s. The higher value of these can be used as a conservative estimate for the total shear velocity u_*, and thus depth-averaged flow velocity U as follows. Figure 7 of Li et al. (2015) allows estimates of dimensionless Chezy friction coefficient $Cz = U/u_*$. The data for gravel-bed and sand-bed rivers is bracketed for the most part by the range Cz = 7 to 20. This suggests that the modified sediment entrainment relation should be valid for flow velocities up to the range 1 – 3 m/s, which are reasonable estimates for bankfull velocity in rivers (Parker, 2014; Birch et al., 2023). The implication is that material in the nominal size range ≥ 1 mm is not subject to significant suspension in typical flood flows of alluvial rivers.
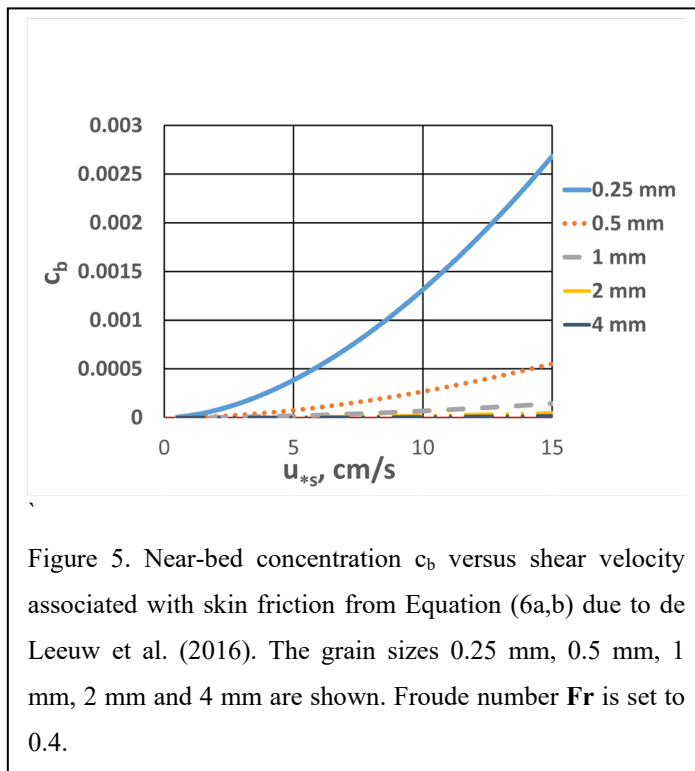
Figure 5. Near-bed concentration c_b versus shear velocity associated with skin friction from Equation (6a,b) due to de Leeuw et al. (2016). The grain sizes 0.25 mm, 0.5 mm, 1 mm, 2 mm and 4 mm are shown. Froude number $\mathbf{Fr}$ is set to 0.4.

The results presented above do not imply that it is physically impossible to suspend gravel. For example, Larsen and Lamb (2016) infer that gravel could be suspended by the megafloods that sculpted the Channeled Scablands, USA. Recently Lin et al. (2022) and Song et al. (2022) have modelled sediment transport in the aftermath of a breach of a high landslide dam in the Himalaya Mountains. Under such conditions, shear velocity was predicted to reach as high as 2 m/s, and mean flow velocity was predicted to reach as high as 10 m/s. Neglecting form drag for the moment, these values applied to the modified Garcia-Parker relation presented here, using a grain size of 4 mm, yields a near-bed concentration taking the maximum possible value of 0.3. This is consistent not only with suspension, but also with the formation of a thick grain flow that can be considered transitional to a debris flow (e.g.

Hernandez-Moreira et al., 2019). Such a grain flow might be indicated in sedimentary rocks in terms of a massive basal unit (Carling, 2013).

5 Pea gravel is preferentially transported as bedload over sand

255   The above analysis provides evidence that pea gravel represents the finest range of approximately spherical gravel that cannot easily be suspended by typical alluvial river flood flows (as opposed to megafloods or flows in steep bedrock streams). The bedload transport rate of a given size D tends to be augmented when it moves over a bed of finer material, as compared to a bed of the same size D. This effect, however, is dependent on absolute size, as well as relative size. Here we return to the thought experiment of Section 3 and consider an example using 4 mm as a characteristic size within

260   the pea gravel range. We argue that a) the bedload transport rate of a grain with size 4 mm moving over a bed of 0.4 mm sand (as opposed to a bed of the same 4 mm material) is augmented to a considerably higher extent than b) the size 40 mm moving over a bed of 4 mm material (as opposed to a bed of the same 40 mm material; Wilcock and Crowe, 2003; Venditti et al. 2010a,b). Wilcock and Crowe (2003) identify 2 mm as a threshold, such that increasing content of material finer than this significantly augments the transport of material coarser than this (GTAS effect).

265   The problem can again be viewed in the context of viscosity. There is abundant evidence that changes in viscosity, e.g., through temperature change, can significantly affect both the transport rate and bedforms in sand-bed streams (e.g., Chen and Nordin, 1976; Southard and Boguchwal, 1990; Nino et al., 2003). Simons and Richardson (1961) have modified a dimensionless bedform regime diagram proposed by Liu (1957), which indicates that the effect of viscosity on bedform regime becomes negligible as particle grain size passes through the range 1.71 – 5 mm (quartz particles on

270   Earth in water at 20°C). Indeed, the effect of viscosity is embedded in the modified Shields relation for the threshold of (significant) bedload transport presented in Garcia (2006). Where τ_c^* denotes a critical Shields number, the threshold condition can be represented as

$$\tau_c^* = \frac{u_{*c}^2}{RgD} = 0.5[0.22\left(D^*\right)^{-0.9} + 0.06\cdot10^{(-7.7(D^*)^{-0.9})}] \tag{6}$$

Here u_{*c} is the shear velocity at the threshold of (significant) motion. Viscosity enters the problem via the definition of

275   dimensionless grain size D^*. For uniform material over a bed of the same size, assuming quartz and water at 20°C, the values of τ_c^* are 0.029 for 40 mm material, 0.024 for 4 mm material and 0.017 for 0.4 mm material. Clearly particles become easier to move as grain size reduces across the pea gravel range. That is, viscosity lubricates a bed that is sufficiently fine, as illustrated analytically in e.g., Ikeda (1982). The issue is discussed in more detail below, and further elaboration is given in the Appendix.

280   But the most important effect for the present analysis concerns how a grain of a given size moves over a bed of finer sizes. Turbulent flows over a granular bed are traditionally divided into a turbulent smooth regime, a turbulent rough

regime and a transitional regime (e.g. Streeter, 1975). Julien and Bounvilay (2013) show data indicating that coarse particles moving over a hydraulically smooth bed do not consistently travel at higher velocities than those traveling over a hydraulic rough bed. They are, however, entrained more easily. Novak and Nalluri (1975) provide convincing experimental evidence that the threshold Shields number for motion of a given grain size is substantially reduced when that particle moves over a hydraulically smooth bed. The viscous sublayer thickness of a turbulent boundary layer can be scaled as (e.g., Garcia, 2006)

$$\delta_v = 11.6 \frac{\nu}{u_{*s}} \tag{7}$$

where δ_v = nominal thickness of the viscous sublayer. Here "nominal viscous sublayer thickness", corresponding to a characteristic length scale for the effect of viscosity, is used in a different sense from "nominal grain size", the latter of which corresponds to Earth-like conditions. Now let u_{*s} = the shear velocity at the threshold of motion u_{*c}. Between Equations (6) and (7), the ratio $(\delta_v/D)_c$, i.e. the value of δ_v/D at the threshold of motion. is found to be:

$$\left(\frac{\delta_v}{D}\right)_c = \frac{11.6}{(D^*)^{3/2} f(D^*)} \quad , \quad f(D^*) = \sqrt{0.5[0.22\left(D^*\right)^{-0.9} + 0.06 \cdot 10^{(-7.7(D^*)^{-0.9})}]} \tag{8}$$

This relation is plotted in Figure 6. Consider first a nominal 40 mm grain moving over a bed of nominal 4 mm material. The value of $(\delta_v/D)_c$ for either grain size is no larger than 0.074, indicating a turbulent rough bed with no role for viscosity. In the case of a 4 mm grain moving over a 0.4 mm bed, $(\delta_v/D)_c$ of the bed is 2.81. This indicates that the 4 mm grain moves over a bed that is transitional to turbulent smooth, and thus is subject to increased mobility via lowered threshold Shields number demonstrated experimentally by Novak and Nalluri (1975).

Novak and Nalluri (1975) offer no explanation for their result that a grain in a turbulent smooth flow has a lower critical Shields number than the same grain in a turbulent rough flow, other than remarking that the result is "to be expected". In the Appendix, we outline a broad-brush theory as to why this should be true. The key parameter is the ratio u_f/u_*, where u_f is the flow velocity averaged over turbulence acting on the grain. This ratio takes an asymptotic value for the limit of turbulent rough flow, but increases monotonically with increasing grain size for turbulent smooth flow, causing the critical Shields number to correspondingly decline monotonically.

The tendencies outlined above are corroborated by the results of Dingle and Venditti (2023), who show, for example, enhanced mobility of clasts of size 3.8 mm as sand of size 0.57 mm occupies an increasing fractional content in the bed surface layer. It should be noted, however, that were bedforms to be present, they would tend to break up the effect of viscosity, as they set an internally-generated roughness (e.g. Lapôtre et al., 2017).

6 "Sand-bed-like" versus "gravel-bed-like" rivers; generalization for Earth, Titan and Mars

For reference, we here repeat the definition of D* given in Equation (1c):

$$D^* = D\frac{(Rg)^{1/3}}{v^{2/3}} \tag{1c}$$

All specific evaluations of D* given above have been for a natural (e.g., granitic) particle (e.g. R = 1.65 for quartz) on Earth (g = 9.81 m/s²) in water at 20°C (ν = 1.00x10⁻⁶ m²/s). These same arguments apply to limestone particles with only modest modification in submerged specific gravity R; here we group these together as "natural particles on Earth." Based on the range 1 – 5 mm, we can loosely divide river reaches into "sand-bed-like" or "gravel-bed-like" depending on whether or not characteristic bed surface size (e.g. D_{50}) is less than or greater than 2 mm. For the above conditions, the size D = 2 mm yields a value of D* = 51. When using this size as an approximate boundary between "sand-like" and "gravel-like" behaviour, however, it must be borne mind that the relevant parameter is the dimensionless one. Even on Earth, the kinematic viscosity of water can vary from a low of 2.94x10⁻⁷ m²/s at 100°C to a high of 1.79x10⁻⁶ m²/s. In addition, Viparelli et al. (2015) have documented the mobility of sediment with submerged specific gravities R ranging from 0.5 to 3. A discriminating value D* = 51 thus corresponds to a range of sizes D from as low as 0.73 mm to as high as 4.42 mm.
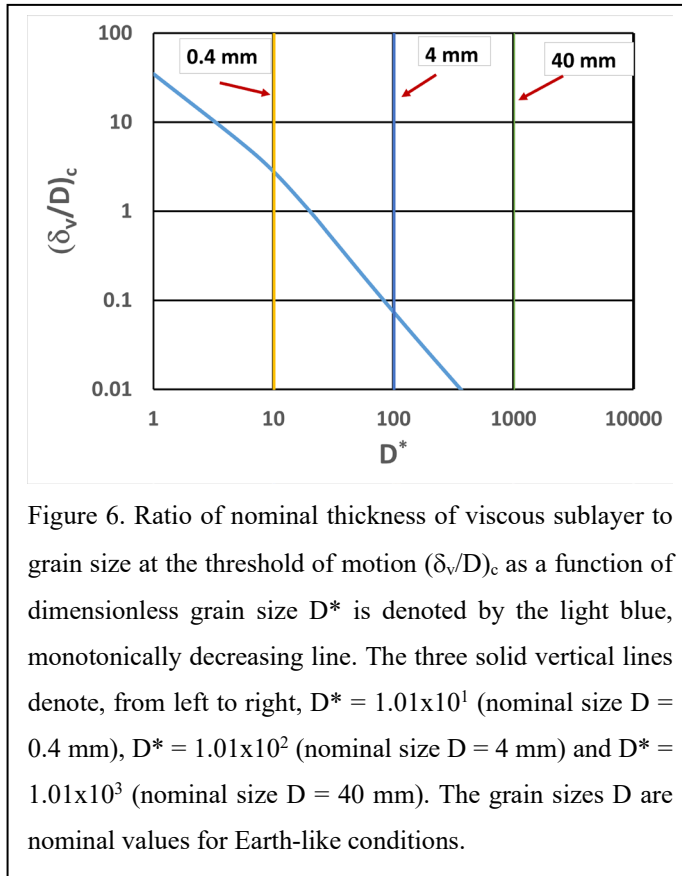
Figure 6. Ratio of nominal thickness of viscous sublayer to grain size at the threshold of motion $(\delta_v/D)_c$ as a function of dimensionless grain size D* is denoted by the light blue, monotonically decreasing line. The three solid vertical lines denote, from left to right, D* = 1.01x10¹ (nominal size D = 0.4 mm), D* = 1.01x10² (nominal size D = 4 mm) and D* = 1.01x10³ (nominal size D = 40 mm). The grain sizes D are nominal values for Earth-like conditions.

We are now able to cast the bedload transport relation of Wilcock and Crowe (2003) in purely dimensionless form. Generalizing from their 2 mm criterion, as the content of grains in the bed with dimensionless size < D* = 51 is increased, the transport of grains with dimensionless size > D* = 51 is enhanced. The formulation is now directly applicable to rivers on Mars and Titan as well as Earth, in so far as it can be applied to a heavenly body with arbitrary gravitational acceleration g, a fluid with arbitrary kinematic viscosity ν, and a sediment particle of arbitrary submerged specific gravity R.

Birch et al. (2023) illustrate how the dimensionless number D* transforms into dimensioned numbers for Mars, where gravitational acceleration is significantly lower, and Titan, where gravitational acceleration is even lower, the clasts are ice rather than quartz and the fluid is a mix of methane and ethane. They show that the discriminator D* = 51 translates

to about 2.66 mm on Mars (mafic sediment in water at 20°C), and 3.16- 4.42 mm on Titan, (ice particles in liquid methane/ethane at 84 - 96°K. Lamb and Venditti (2016) present a similar calculation.

345 We emphasize here that the nominal dimensioned size 2 mm is used as shorthand for the narrow range 1 – 5 mm corresponding to natural particles (e.g. granitic or limestone) on Earth in water at 20°C. The corresponding dimensionless range for D*, which we argue to be more universal, is 25 – 126.

7 Discussion

We do not present the above analysis in the context of a specific morphodynamic model. Instead, the analysis bears
350 on the physics underlying what Church and Hassan (2023) describe as a "clear tendency for grains in the range 1–8 mm to outrun both larger and smaller grains in the condition of size-selective transport" via bedload (rather than suspended load) transport. This tendency can in turn be related to the evolution of the pea-gravel grain size gap in the bed surface layer of a long profile of a net-depositional river, as expressed in terms of the bed material sizes D_{50} and D_{60} shown in Figure 2a,b. Pea gravel is not easily suspended, but can be preferentially moved as bedload over a coarser bed (weight
355 versus hiding-exposure effect) as well as a finer bed (hydrodynamic smoothing effect). The implication is that even if there is no grain size gap in the feed sediment, the pea gravel tends to become diluted over a long reach, as described in the following thought experiment.

We assume a long river reach undergoing deposition. The grain size distribution of the deposit contains three size ranges: a "sand" range, a "pea gravel range" and a "coarse gravel range". We further specify that the fraction of material
360 in each of the three ranges is equal: 1/3 "sand", 1/3 "pea gravel" and 1/3 "coarse gravel". We divide the reach into upstream and downstream segments of equal length. Let the upstream deposit be 2/3 "coarse gravel" and 1/3 "pea gravel", and the downstream deposit be 2/3 "sand" and 1/3 "pea gravel". The total amount of the deposit in each size range is equal. Yet the median size D_{50} of the deposit must abruptly drop from the "coarse gravel" size to the "sand" size halfway down the reach. No paucity of pea gravel is necessary for such behaviour. Instead, the pea gravel is diluted due
365 to its preferential mobility as bedload compared to coarser and finer sediment. A first attempt to incorporate the above ideas into a morphodynamic model is given in An et al. (2020).

In the analysis above, grain size D is interpreted as an equivalent diameter of a sphere. The analysis would require modification for grain shapes that deviate significantly from spherical. The fall velocity relation of Dietrich (1982) includes a correction factor for grain shape. Particles with a plate-like shape may be significantly easier to suspend than
370 spheres. The arguments above do not rely on the assumption of grain abrasion. Abrasion may, however, play a role in the evolution of some sharp gravel-sand transitions.

The mobilization effect observed when sand is added to a gravel bed, without major change in bed slope, has been verified experimentally by Cui et al. (2003a) and Dingle and Venditti (2023). Lamb et al. (2008) indicate that the critical Shields number of sediment increases with bed slope. In the original experiments of Wilcock and Crowe (2003), where

375   the flow was allowed to reach mobile-bed equilibrium, a higher sand content correlated with a lower bed slope. The evolution of this lower slope may also be combined with the tendency for critical Shields stress to be slope-dependent (Lamb et al., 2008). This slope effect is included in the bedload transport relation of Schneider et al. (2015).

    The present analysis is focused on the mobility of grains in the pea gravel range. It has been demonstrated above that this grain size range shows little tendency to be suspended even at flood stage in natural alluvial rivers. Thus the present

380   arguments can be posed in the context of bedload transport. The analysis is applicable to, but does not provide a complete explanation of the formation of gravel-sand transitions, for which the transport and deposition of sand must be considered as well (Lamb and Venditti, 2016).

8 Conclusions

    The analysis presented here does not specifically identify the size D = 2 mm itself as special. Instead, it serves as

385   shorthand for the dimensionless size D* = 51, and the dimensionless range D* = 25.2 - 126, corresponding to nominal size range of pea gravel ranging from 1 – 5 mm (e.g., granitic or limestone particles on Earth in water at 20°C). We show that this range corresponds to the finest sizes that cannot be significantly transported in suspension in typical floods (~ bankfull flow) of alluvial rivers. In addition, we show that pea gravel is preferentially moved as bedload, both over a coarser gravel bed and a sand bed (at least in the absence of bedforms). The physics of the problem is embodied in the

390   dimensionless grain size D*, which contains kinematic viscosity. These conclusions have bearing on the formation of gravel-sand transitions, because they imply that even in the absence of abrasion or a grain size gap in the feed sediment, pea gravel is subject to dilution within any long depositional reach along which downstream fining is observed. That is, pea gravel intrinsically "has trouble finding a home" where it can dominate in the sediment deposit.

    The formulation is directly applicable to Mars, where gravitational acceleration is lower than Earth, and Titan, where

395   the gravitational acceleration is even lower, the particles in transport are ice rate than e.g., quartz, and the fluid is mixture of methane and ethane rather than water.

Appendix

    Novak and Nalluri (1975) use experimental data to show that a grain placed on the bed of a flow in the turbulent smooth range has a substantially lower critical Shields number than the same grain placed on the bed of a flow in the

400   turbulent rough range (their Figure 2). They do not, however, show a theoretical analysis justifying this conclusion. Here we present a broad-brush analysis to illustrate the general physics behind this behaviour. A sphere of size D is placed on the bed of a channel. Where z is an upward normal coordinate from the bed, u is streamwise flow velocity over averaged over turbulence and k_s is roughness height, the distribution of flow velocity over the bed takes the following form for turbulent rough flow;

405
$$\frac{u}{u_*} = 2.5 \, \ell n\left(\frac{z}{k_s}\right) + 8.5 \qquad (A1a)$$

(e.g. Schlichting, 1968). Here we crudely estimate k_s as equal to D. The corresponding form for turbulent smooth flow is;

$$\frac{u}{u_*} = \begin{cases} \dfrac{u_* z}{\nu} \quad, \quad \dfrac{u_* z}{\nu} \leq 11.6 \\[2ex] 2.5 \, \ell n\left(\dfrac{u_* z}{\nu}\right) + 5.5 \quad, \quad \dfrac{u_* z}{\nu} > 11.6 \end{cases} \qquad (A1b)$$

(e.g. Schlichting, 1968). For simplicity, we do not consider flow that is transitional between the turbulent smooth and turbulent rough regimes.

410   The flow velocity u_f acting on the grain is evaluated at the top of the particle, here approximated as $z = D$. It follows from these definitions and Equation (A1a) that in the turbulent rough case, the ratio $F_u = u_f/u_*$ can be estimated as

$$F_u = \frac{u_f}{u_*} = 8.5 \qquad (A2a)$$

In the turbulent smooth case, from Equation (A1b) it is found that

$$F_u = \frac{u_f}{u_*} = \begin{cases} 11.6\dfrac{D}{\delta_v} \quad, \quad \dfrac{D}{\delta_v} \leq 1 \\[2ex] 2.5\ell n\left(11.6\dfrac{D}{\delta_v}\right) + 5.5 \quad, \quad \dfrac{z}{\delta_v} > 1 \end{cases} \qquad (A2b)$$

415   where δ_v is the nominal viscous sublayer thickness given by Equation (7).

The drag force F_D and Coulomb resistive force F_R are estimated as follows:

$$F_D = \frac{1}{2}\rho c_D\left(\frac{D}{2}\right)^2 u_f^2 \quad, \quad F_R = \frac{4}{3}\mu_c\rho Rg c_D\left(\frac{D}{2}\right)^3 \qquad (A3a,b)$$

where c_D is the dimensionless drag coefficient on a sphere and μ_c is a dimensionless coefficient of Coulomb friction. Again for simplicity, we neglect any lift force on the particle, and express the threshold of motion in terms of the
420   condition

$$F_D = F_R \qquad (A4)$$

Reducing between Equations (A3) and (A4), the critical shear velocity u_{*c} and critical Shields number $\tau_c^* = u_{*c}^2/(RgD)$ at the threshold of motion are given as

$$\tau_c^* = \frac{u_{*c}^2}{RgD} = \frac{4}{3}\frac{\mu_c}{c_D F_u^2} \qquad (A5)$$

425   We evaluate the drag coefficient as a function of the fluid Reynolds number acting on the particle $\mathbf{Re} = u_f D/\nu$ using the explicit functional relation of Goldstein (1929), as quoted in Yang et al. (2015);

$$c_D = \frac{24}{\mathbf{Re}}\left[1 + \frac{\frac{3}{16}\mathbf{Re}}{1 + \frac{\frac{19}{240}\mathbf{Re}}{1 + \frac{1}{122}\mathbf{Re}}}\right] \quad , \quad \mathbf{Re} = \frac{u_f D}{\nu} \tag{A6}$$

This relation is accurate from the Stokes range out to $\mathbf{Re} = 1\times10^5$.

       For the case of a grain on the bed of a turbulent rough flow, we assume an angle of repose of 35°, or thus a coefficient

430   of Coulomb friction $\mu_c = 0.7$. In the extreme case of turbulent rough flow at a value $\mathbf{Re}$ that is large enough for the drag coefficient c_D to asymptote out to the Reynolds-independent value of 0.422 of Equation (A6), Equations (A2a), (A5) and (A6) yield the simple result

$$\tau_c^* = 0.0306 \tag{A7}$$

This value is very close to the asymptotic value 0.030 from Equation (6) obtained for large D*.

    In principle, the coefficient of Coulomb friction over a smooth bed ought to be less than the value over a rough bed. But this is a geometric rather than a hydrodynamic effect, so we keep μ_c constant in estimating the threshold Shields number for a grain placed on the bed of turbulent smooth flow. Between Equations (A1b), (A2b), (A5) and (A6), the critical Shields number τ_c^* can be represented in terms of the ratio D/δ_v as shown in Figure A1 (solid line labelled "present relation"). Also shown therein is the asymptotic result of Equation (A7) for a sufficiently coarse grain subjected to turbulent rough flow (dashed line labelled "turbulent rough limit"), and the empirical Equation (13) of Novak and Nalluri (1975) for the threshold of motion over a
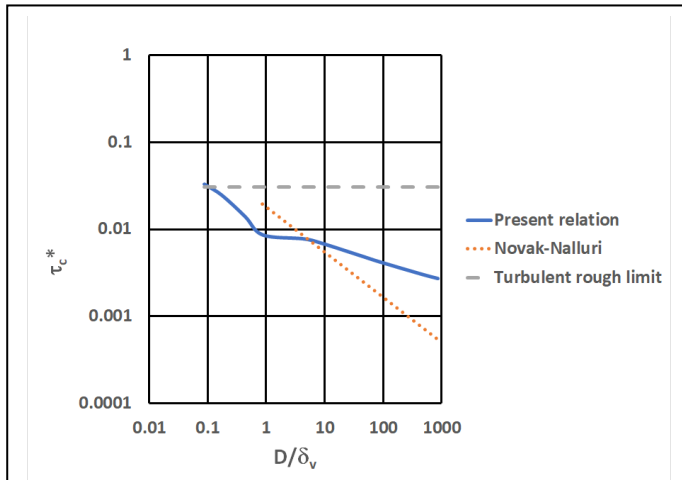
Figure A1. Critical Shields number τ_c^* as a function of the ratio D/δ_v, i.e. the ratio of grain size versus the nominal thickness of the viscous sublayer. Shown above are the relation for the limit of turbulent rough flow, the empirical relation of Novak and Nalluri (1975) for turbulent smooth flow, and the relation derived herein (present relation) for turbulent smooth flow.

smooth bed (labelled "Novak-Nalluri"). While the present relation, broad-brush as it is, does not precisely reproduce the empirical result of Novak and Nalluri (1975), it serves to illustrate that a) a grain on a bed with turbulent smooth flow has a lower threshold Shields number than the same grain on a bed with turbulent rough flow, and b) all other factors equal, the larger the grain size, the larger becomes the difference between the two.

455   The reason for this difference in behaviour is, for the most part, bound up in the ratio F_u of flow velocity acting on the grain u_f to shear velocity u_*. For turbulent rough flow, F_u takes the value 8.5 in the present analysis (Equation A2a). For turbulent smooth flow, F_u increases monotonically with grain size according to Equation (A2b). Since the term F_u occurs in the denominator of Equation (A5) as grain size increases, the critical Shields number accordingly decreases monotonically in the turbulent smooth case.

460   It is of some value to note that analysis similar to the one above, but applied for grain size mixtures solely in the turbulent rough regime, yields the hiding-exposure function of Egiazaroff (1965), which is embedded in modified form in the bedload transport relation of Ashida and Michiue (1972).

465 **Table A1. Notation**

Here [1] denotes the dimensions of unity (dimensionless).

A   Constant in Equation (1a) [1]

c_b near-bed equilibrium volume concentration of suspended sediment [1]

c_D drag coefficient on a sphere [1]

470 D   grain size [L]

D_{50} median grain size of bed surface [L]

D_{60} grain size such that 60 percent of bed surface material is finer [L]

D^* $= (Rg)^{1/3}D/\nu^{2/3}$; dimensionless grain size [1]

F_D drag force on a sediment grain on a bed [MLT^{-2}]

475 F_R Coulomb resistive force on a sediment grain on a bed [MLT^{-2}]

Fr $= U/(gH)^{1/2}$, Froude number [1]

F_u $= u_f/u_*$ [1]

g   acceleration of gravity [L/T^{-2}]

H   flow depth [L]

480 k_s bed roughness height [L]

R $= (\rho_s - \rho)/\rho$; submerged specific gravity of sediment [1]

Re $u_f D/\nu$ [1]

$\mathbf{Re}_{vp}$ $= v_s D / \nu$ [1]

$\mathbf{R}_f$ dimensionless fall velocity of sediment [1]

U   depth-averaged flow velocity $[LT^{-1}]$

u   local streamwise flow velocity averaged over turbulence [L]

u_f local value of u acting on a grain on the bed [L]

u_* shear velocity $[LT^{-1}]$

u_{*c} shear velocity at threshold of motion $[LT^{-1}]$

u_{*s} shear velocity due to skin friction $[LT^{-1}]$

v_s fall velocity of sediment $[LT^{-1}]$

X   parameter defined by Equation (5b) [1]

z   distance upward normal to the bed [L]

Z_u parameter defined by Equation (1b), Equation (4b) [1]

δ_v nominal thickness of viscous sublayer [L]

μ_c Coulomb coefficient of friction associated with a grain on a bed [1]

ν kinematic viscosity of fluid (water or methane-ethane mixture) $[L^2T^{-1}]$

ρ density of fluid (water or methane-ethane mixture) $[ML^{-3}]$

ρ_s density of sediment (quartz, limestone, ice particles etc.) $[ML^{-3}]$

τ_c^* critical Shields number for the onset of significant sediment transport [1]

Competing interests

The contact author has declared that none of the authors has any competing interests.

Acknowledgements

The participation of Parker was aided by funding from the W. H. Johnson Chair of the Department of Earth Sciences and Environmental Change, University of Illinois Urbana-Champaign, USA. and also by Tsinghua University China through a colleague, Xudong Fu. The participation of Chenge An was supported by the National Natural Science Foundation of China (grant 52009063) and the Young Elite Scientists Sponsorship Program of CAST (grant 2021QNRC001). Michael Church provided valuable comments which have been incorporated into the text. The authors acknowledge helpful reviews from Enrica Viparelli and an anonymous referee.

References

An C., Parker G., Fu X., Lamb M. P., Venditti J. G.: Morphodynamics of downstream fining in rivers with unimodal sand-gravel feed, Proceedings International Conference on Fluvial Hydraulics (River Flow 2020), Delft, Netherlands, July 7-10, 2020.

515 Ashida, K. and Michiue, M.: 1972, Study on hydraulic resistance and bedload transport rate in alluvial streams, Transactions, Japan Soc. Civil Eng., 206 (in Japanese).

Birch, S.P.D., Parker, G., Corlies, P., Soderblom, J., Miller, J.W., Palermo, R., Lora, J.M., Ashton, A.D.,, Hayes. A.G., and Perron, J.T.: Reconstructing river flows remotely on Earth, Titan, and Mars. Proc. Nat. Acad. of Sciences (USA), 120(29), 2023.

520 Brownlie, W. R.: Prediction of flow depth and sediment discharge in open channels, Report No. KH-R-43A, W. M. Keck Laboratory of Hydraulics and Water Resources, California Institute of Technology, Pasadena, California, USA, 1981, available at https://thesis.library.caltech.edu/5064/3/brownlie_wr_1982.pdf.

Butler, J.: Further reflections on conversations of our time, Diacritics 27 (spring), 1997.

Carling, P.A.: Freshwater megaflood sedimentation: What can we learn about generic processes? Earth-Science Reviews
525 125, 87-113, 2013.

Chen, H. Y., and Nordin, C. F Jr.: Missouri river temperature effects in the transition from dunes to plane bed, U. S. Army Engineer District, Omaha December 1976. 41 p. M. R. D. Sediment Series 14 1976.

Church, M. and Hassan, M. A.: The fluvial grain size gap: experimental confirmation of hydraulic origin. Earth. Surf. Processes and Landforms, https://doi.org/10.1002/esp.5562, 2023.

530 Cui, Y., Parker, G., Lisle, T., Gott, J., Hansler, M., Pizzuto, J. E., Allmendinger, N. E. and Reed, J. M.,Sediment pulses in mountain rivers. Part 1. Experiments. Water Resources Research, 39(9), 2003a.

Cui, Y., Parker, G., Pizzuto, J. E. and Lisle, T. E: Sediment pulses in mountain rivers. Part 2. Comparison between experiments and numerical predictions. *Water Resources Research*, 39(9), 2003b.

Dietrich, W. E.: Settling velocity of natural particles, Water Res. Res., 18(6), 1982.

535 Dingle, E.H. ,Kusack, K. M and Venditti J. G.: The gravel-sand transition and grain size gap in river bed sediments. Earth Science Reviews, 222, 2021.

Dingle, E. H. and Venditti, J. G.: Experiments on the grain size gap in river bed sediments: Abstract European Geophysical Union, EGU23-7423, 2023.

Dong, T., Nittrouer, J.A., Il'echiva, E., Pavlov, McElroy, B, M., Czapiga. M., Ma, H.B. and Parker, G.: Controls on gravel
540 termination in seven distributary channels of the Selenga River delta, Baikal Rift basin, Russia. Geol. Soc. Am. Bull., 128(7-8), 2016.

Egiazaroff, I. V.: Calculation of nonuniform sediment concentrations, J. Hydraul. Engrg., 91(4), 1965.

Engelund, F. and Hansen, E.: A Monograph on Sediment Transport in Alluvial Streams, Technisk Vorlag, Copenhagen, Denmark, 1967.

545   Ferguson, R., Hoey, T., Wathen, S., and Werritty, A.: Field evidence for rapid downstream fining of river gravels through selective transport, Geology 24(2), 1996.

Frings, R. M.: Sedimentary characteristics of the ravel-sand transition in the River Rhine: J. Sed. Res., 81, 2011.

Fujita, K., Yamamoto, K. and Akahori, Y,: Evolution mechanisms of the longitudinal bed profiles of major alluvial rivers in Japan and their implications for profile change prediction, Proc. Japan Soc. Civil Eng. 600(II-44) 1998 (in Japanese).

550   Garcia, M. H.: ASCE Manual of Practice 110 — Sedimentation Engineering, American Society of Civil Engineering, 2006.

Garcia, M. H. and Parker, G.: Entrainment of bed sediment into suspension, J. Hydraul. Engrg, 117(4), 414 435, 1991.

Goldstein, S.: The steady flow of a viscous fluid past a fixed spherical obstacle at small Reynolds numbers, Proc. Roy Soc A, 225-235, 1929.

Guy, H. P, Simons, D. B. and Richardson, E. V.: Summary of alluvial channel data from flume experiments, 1956-61, U. S.
555   Geol. Survey Prof. Paper 462-I, 1966.

Haljasmaa, I. V.: On the drag of fluid and solid particles freely moving in a continuous medium. Doctoral Dissertation, University of Pittsburgh, 2006.

Hey, R, D., Bathurst, J. C and Thorne, C. R.: Gravel-bed Rivers, 1985, J. Wiley, 1982.

Hernandez-Moreira, R., Jafarinek, S, Sanders, S., Kendall, C. G. St., Parker, G and Viparelli, E.: Emplacement of massive
560   deposits by sheet flow, Sedimentology 67(4), 2019.

Hill, K. M., Gaffney, J. Baumgardner, S., Wilcock, P. and Paola, C.: Experimental study of the effect of grain sizes in a bimodal mixture on bed slope, bed texture, and the transition to washload, Water. Res. Res, 53(1), 2016.

Ikeda, S.: Lateral bed load transport on side slopes, J. Hydraul. Engrg. 128(1), 1982.

Julien, P. Y and Bounvilay, B.: Velocity of rolling bed load particles, J. Hydraul. Engrg, 139(2), 2013.

565   Jutzeler, M., McPhie, J, Allen, J. R. and Proussevitch, A. A.: Grain size distribution of volcaniclastic rocks 2: Characterizing grain size and hydraulic sorting, Jour. Volcanology and Geothermal Research, 301(15), 191-203, 2015.

Khosravi, K., Khozani, Z. S, nd Cooper, J. R.: Predicting stable gravel-bed river hydraulic geometry: A test of novel, advanced, hybrid data mining algorithms, Envir. Modelling & Software, 144, 2021.

Kodama, Y. Downstream changes in the lithology and grain size of fluvial gravels, the Watarase River, Japan; evidence of
570   the role of abrasion in downstream fining, J. Sed. Res., 64(1a), 1994.

Lamb, M. P, Dietrich, W. E., and Venditti, J. G.: Is the critical Shields stress for incipient sediment motion dependent on channel-bed slope? Jour. Geophys. Res. Earth Surface, 113 (F2), 2008.

Lamb, M. P. and Venditti, J. G.: The grain size gap and abrupt gravel-sand transitions in rivers due to suspension fallout, Geophys. Res. Letters, 43(8), 2016.

575   Lapôtre, M.G.A., Lamb, M.P. and McElroy B.J.: What sets the size of current ripples?, Geology, 45(3), doi:10.1130/G38598, 2017.

Laronne, J. B. and Tsutsumi, D.: Special Issue: Gravel Bed Rivers 8, Special Issue, Earth Surf. Processes and Landforms, 2018.

Larsen, I.J. and Lamb, M. P.: Progressive incision of the Channeled Scablands by outburst floods, Nature, doi:10.1038/nature19817, 2016.

de Leeuw, J., Lamb, M. P., Parker, G., Moodie, A. J., Haught, D., Venditti, J. G. and Nittrouer, J. A. Entrainment and suspension of sand and gravel. Earth Surf Dynam., 8(2), 2020.

Li, C., Czapiga, M. J., Eke, E. C., Viparelli, E. and Parker, G.: Variable Shields number model for river bankfull geometry: bankfull shear velocity is viscosity-dependent but grain size-independent, J. Hydraul. Res. 53, 2015.

Li, Shun-Li, Li, Shen-Li, Shan, X., Gong, C-L and Yu, X-H.: Classification, formation, and transport mechanisms of mud clasts, International Geology Review 59(12), 1609-1620, 2017.

Lin, Y-P, An, C-G, Parker, G., Liu, W-M and Fu, X-D: Morphodynamics of bedrock-alluvial rivers subject to landslide dam outburst floods, J. Geophy, Res. Earth Surfaces 127(9), 2022.

Lin, Y-P, An, C-G, Zheng, S., Nie, R-H, Parker, G., Hassan, M. A, Czapiga, M. J. and Fu, X-D: Degradation of a foreland river after the Wenchuan Earthquake, China: a combined effect of weirs, sediment supply and sediment mining, Water Resources Research 59(10), 2023.

Liu, H. D: Mechanics of Sediment Ripple Formation, Proceedings American Society of Civil Engineers, ASCE, 83 (HY2), 1197–1 to 1197–23, 1957.

Meyer-Peter, E. and Müller, R.: Formulas for Bed-Load Transport, Proceedings, 2nd Congress, International Association of Hydraulic Research, Stockholm, 39-64, 1948.

Nino, Y., Lopez, F. and Garcia, M. H.: Threshold for particle entrainment into suspension, Sedimentology, 50, 247–263, 2003.

Novak, P. and Nalluri, C.: Sediment transport in smooth fixed bed channels, J. Hydraul. Engrg., 101(9), 1975.

Paola, C and Seal, R.: Grain size patchiness as a cause of selective deposition and downstream fining, Water Resources Research, 31(5), 1995.

Parker, G. and Klingeman, P.: On why gravel bed streams are paved. Water Resources Research, 18(5), 1409 1423, 1982.

Parker, G.: Surface based bedload transport relation for gravel rivers, J. of Hydraul. Res., 28(4), 1990.

Parker, G. and Toro-Escobar, C. M: Equal mobility of gravel in streams: the remains of the day. Water Resources Research, 38(11), 1264, doi:10.1029/2001WR000669, 2002.

Parker, G.: Dimensionless Bankfull Hydraulic Relations for Earth and Titan. Am. Geophys. Union Fall Meeting, abstract id.H31G-06, 2005, presentation available at:
http://hydrolab.illinois.edu/people/parkerg/_private/SeminarsPosters/GrailTitanAGU05.pdf

Parker, G., Wilcock, P., Paola, C., Dietrich, W. E. and Pitlick, J.: Quasi-universal relations for bankfull hydraulic geometry of single-thread gravel-bed rivers, J. Geophys. Res. Earth Surface, 112(F4), 2007.

610 Parker, G.: Teasing out simplicity from complexity: the law of constant bankfull velocity in alluvial rivers. Am. Geophys. Union Fall Meeting, 2014, abstract id. EP41D-06, 2014.

Peng, H., Huang, H-Q, Yu, G-A and Zhong, H. W.: Applicability of flow resistance formulae for sand-bed channels: an assessment using a very large data set, Front. Environ. Sci., 16, 2022

van Rijn, L. C. Sediment transport, part I:bed load transport, J. Hydraul. Engrg. 110(10), 1984.

615 Rouse, H.: Experiments on the mechanics of sediment suspension, Proceedings 5th International Congress on Applied Mechanics, Cambridge, Mass,, 550-554, 1939.

Sambrook Smith, G. H. and Ferguson, R. I.; The gravel-sand transition along river channels. J Sed. Research, 65(2a), 1995.

Schlichting, H.: Boundary Layer Theory, 7th Ed., McGraw-Hill, New York, 1979.

Schneider, J. M., Rickenmann, D., Turowski, J. M, Bunte, K. and Kirchner, J. W.: Applicability of bed load transport models
620 for mixed size sediments in steep streams considering macro-roughness, Water Resour. Res., 51, 5260–5283, 2015.

Shaw, J. and Kellerhals, R.: The Composition of Recent Alluvial Gravels in Alberta River Beds, Bulletin 41, Alberta Research Council, Edmonton, Alberta, Canada, 1982.

Simons, D. B., and Richardson, E. V.: Forms of bed roughness in alluvial channels, Journal of the Hydraulics Division, ASCE, 87(3), 87–105, 1961.

625 Song Y., Fu X., Lin Y., An C., Ma H.: What controls the magnitude and the shape of landslide dam-breaching flood hydrograph? Case studies of emergent forecasts for outburst floods of Jiala and Baige Barrier Lakes, Frontiers in Water, 4: 834132. DOI: 10.3389/frwa.2022.834132, 2022.

Southard, J. B. and Boguchwal, L. A.: Bed configurations in steady unidirectional water flows; Part 3, Effects of temperature and gravity, J. Sed. Res. 60(5), 1990.

630 Streeter, V. L.: Fluid Mechanics, McGraw-Hill, 741 p., 1971.

Tucker, M. E.: Sedimentary Rocks in the Field. J. Wiley, Third Edition, 232 p. 2003.

Venditti, J. G., Dietrich, W. E. Nelson, P. A., Wydzga, M. A., Fadde, J. and Sklar, L.: Mobilization of coarse surface layers in gravel-bedded rivers by finer gravel bed load, Water Resour. Res., 46, W07506, doi:10.1029/2009WR008329, 2010a.

Venditti, J. G., Dietrich, W. E., Nelson, P. A., Wydzga, M. A., Fadde, J. and Sklar, L.: Mobilization of coarse surface layers
635 in gravel-bedded rivers by finer gravel bed load, Water Res. Res., 46(7), 2010b.

Venditti, J. G. and Church, M.: Morphology and controls on the position of a gravel-sand transition: Fraser River, British Columbia, J. Geophys. Res. Earth Surface, 119, 2014.

Venditti, J. G. Domarad, N., Church, M. and Rennie. C. D. The gravel-sand transition: Sediment dynamics in a diffuse extension, J. Geophys. Res. EarthSurf., 120, doi:10.1002/2014JF003328, 2015

640 Venditti, J. G. and Bradley, R.: Bedforms in sand bed rivers, in Treatise on Geomorphology, Academic Press, 2022.

Viparelli, E. Solari, L and Hill, K. M.: Downstream lightening and upward heavying: Experiments with sediments differing in density, Sedimentology, 62(5), 2015.

Wilcock, P. R. and Crowe, J. C.: Surface-based transport model for mixed-size sediment, J. Hydraul. Engrg, 129(2), 2003.

645 Wilkerson, G. V. and Parker, G.: Physical basis for quasi-universal relations describing bankfull hydraulic geometry of sand-bed Rivers, J. Hydraul. Engrg., 137(7), 2011.

Wright, S. and Parker, G.: Flow resistance and suspended load in sand-bed rivers: simplified stratification model, J. Hydraul. Engrg, 130(8), 796-805, 2004.

Xu, J-X: Comparison of hydraulic geometry between sand- and gravel-bed rivers in relation to channel pattern discrimination, Earth Surf. Processes and Landforms, 29, 2004.

650 Yang, H-L, Fan M-Q, Liu, A-R and Dong, L-P: General formulas for drag coefficient and settling velocity of sphere based on theoretical law, Intl. Jour. Mining Science and Tech., 25(2), 219-223, 2015.

Yatsu, E.: On the longitudinal profile of the graded river, Trans. Am. Geophys. Union, 36 1955.